Am J Cancer Res 2025;15(8):3434-3448
www.ajcr.us /ISSN:2156-6976/ajcr0167012

Original Article

Differentiating early-stage nasopharyngeal carcinoma from adenoidal hypertrophy via SLC40A1 expression and developing a prognostic model for disease progression

Hongwei Wang[1,3], Suqing Qi[1,3], Chaobing Liu[2,3], Zhenhua Qiao[2,3], Chao Zhang[1,3]

[1]Department of Stomatology, Hebei Eye Hospital, Xingtai 054001, Hebei, China; [2]Department of Otolaryngology, Hebei Eye Hospital, Xingtai 054001, Hebei, China; [3]Hebei Provincial Clinical Research Center for Eye Diseases, Hebei Eye Hospital, Xingtai 054001, Hebei, China

Received June 23, 2025; Accepted August 4, 2025; Epub August 15, 2025; Published August 30, 2025

Abstract: Objective: To investigate the expression and diagnostic utility of solute carrier family 40 member 1 (SLC40A1) in differentiating early diagnosis of nasopharyngeal carcinoma (NPC) from adenoid hypertrophy (AH), and to develop a prognostic prediction model based on its expression. Methods: Public databases were used to analyze SLC40A1 expression in head and neck squamous cell carcinoma (HNSC) and its association with prognosis, pathological staging, and immune infiltration. A total of 102 NPC patients, 97 AH patients, and 101 healthy controls were enrolled between October 2021 and October 2023. SLC40A1 expressions in tissues and serum were assessed via real-time reverse transcription polymerase chain reaction and Western blotting. Associations with clinicopathological features were evaluated. Receiver operating characteristic (ROC) curves evaluated diagnostic performance. Logistic regression identified prognostic factors, and a predictive model was constructed. Results: Bioinformatics analysis indicated downregulated SLC40A1 in HNSC, negatively associated with tumor (T) stage and distant metastasis (M) stage. Clinical validation showed significantly lower SLC40A1 mRNA and protein levels in NPC compared to AH and controls, with negative correlation to Epstein-Barr virus (EBV) infection (all $P<0.05$). Serum SLC40A1 mRNA demonstrated 90.20% sensitivity and 62.38% specificity for NPC diagnosis. When combined with EBV DNA, it yielded an improved diagnostic performance (AUC=0.913). Tumor diameter >5 cm and lymph nodes ≥2 were independent risk factors for NPC progression, while high SLC40A1 expression was protective (OR=0.140, 95% CI: 0.028-0.700). The final model achieved 91.67% sensitivity and 72.00% specificity (AUC=0.863). Conclusion: SLC40A1 is significantly downregulated in NPC and may serve as a diagnostic and prognostic biomarker, especially when combined with EBV status.

Keywords: Nasopharyngeal carcinoma, SLC40A1, adenoidal hypertrophy, diagnostic biomarker, prognosis

Introduction

Nasopharyngeal carcinoma (NPC), originating from the mucosal epithelium of the nasopharynx, is the most common malignancy in otolaryngology and demonstrates distinct regional distribution, with particular high prevalence in Southeast Asia [1]. Although NPC accounts for only approximately 0.7% of all malignant neoplasms globally, its incidence can rise to 30 cases per 100,000 individuals in endemic regions, and this figure has shown an upward trend in recent years [2, 3]. Despite the well-recognized importance of "early detection and early treatment" for malignancies such as NPC, around 70% of patients are still diagnosed at advanced stages [4], leading to poor clinical outcomes in the majority. The main challenge in early NPC diagnosis lies in its insidious and nonspecific clinical presentation, often limited to intermittent nasal obstruction or tinnitus [5]. Moreover, nasopharyngoscopic features in early-stage NPC closely resemble those of adenoidal hypertrophy (AH), making differential diagnosis particularly difficult [6]. Currently, serological testing remains the primary method for distinguishing NPC from AH, especially through Epstein-Barr virus (EBV)-related antibodies such as VCA-IgA and EBNA1-IgA [7]. However, these biomarkers have notable limitations. For instance, while VCA-IgA offers moderate diagnostic value, its positivity rate is only

https://doi.org/10.62347/ZBIH5385

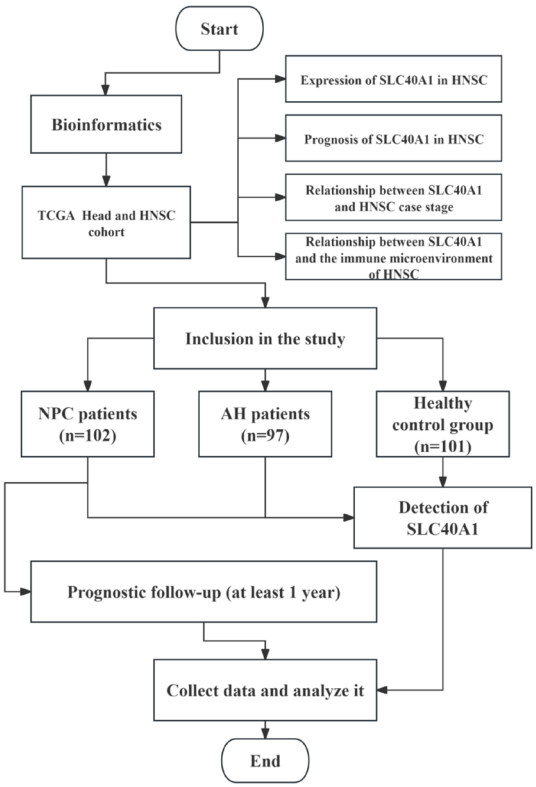

Figure 1. Flow chart of the study. Note: NPC: nasopharyngeal carcinoma, AH: adenoid hypertrophy, HNSC: head and neck squamous cell carcinoma, SLC40A1: solute carrier family 40 member 1.

60%-70% in early-stage NPC. In contrast, children with AH may exhibit false-positive results due to primary EBV infection [8]. Although EBNA1-IgA has high specificity, approximately 10%-15% of NPC patients - especially those in early-stages or with non-keratinizing histology - show low titers or negative results, contributing to missed diagnoses [9]. Furthermore, neither serological marker reflects tumor biology or offers predictive value for disease progression. Thus, identifying novel molecular markers and constructing multidimensional diagnostic models are crucial to improving the differentiation of NPC and AH and guiding more accurate clinical decision-making.

Identifying early-stage NPC through potential molecular biomarkers is currently a key focus of research. For instance, Li et al. identified KLK11 as a potential biomarker for NPC diagnosis and prognosis assessment [10]. Similarly, Zhang et al. found that plasma-circulating CircUNP98 exhibited excellent diagnostic performance for NPC [11]. More recently, Zou et al. identified 12 novel immune-related methylated genes in their analysis of NPC biomarkers [12]. Among these, solute carrier family 40 member 1 (SLC40A1), a crucial iron-transporting protein, attracted particular attention. Abnormal expression of SLC40A1 can disrupt cellular iron metabolism and lead to mitochondrial dysfunction [13]. Dysregulation of iron metabolism in NPC has been well-documented, playing a significant role in disease progression and influencing its radiosensitivity [14-16]. These findings position SLC40A1 as a potential clinical marker for NPC. However, further in-depth studies are needed to confirm the exact relationship between SLC40A1 and NPC.

Consequently, this study aims to conduct a preliminary analysis of the clinical significance of SLC40A in NPC and assess its potential value in evaluating disease severity, with the goal of providing new insights and guidelines for the future diagnosis and treatment of NPC.

Materials and methods

Study design

This study was designed as a retrospective analysis involving patients with NPC, individuals with AH, and healthy volunteers who visited Hebei Eye Hospital between October 2021 and October 2023. To determine the required sample size, the G-power software (v3.1.9.2) was employed. The following parameters were set: an effect size of 0.3 (with values approaching 0.5 indicating the need for larger sample sizes as the study scale increases), an alpha (α) error probability of 0.05, and a statistical power of 0.90. The calculations indicated that a minimum of 88 participants per group was required. This study was approved by the Ethics Committee of Hebei Eye Hospital (approval number: 2024KY2501) and conducted in strict accordance with the *Declaration of Helsinki*. A detailed study flowchart is provided in **Figure 1**.

Bioinformatics analysis

We retrieved the standardized pan-cancer dataset from the University of California, Santa Cruz database, specifically the head and neck squamous cell carcinoma (HNSC) cohort from the cancer genome. The gene expression profiles for SLC40A1 (ENSG00000138449) were extracted for each sample. These expression

Table 1. Sequence of primers

	F (5'-3')	R (5'-3')
SLC40A1	AACAAGCACCTCAGCGAGAG	CACATCCGATCTCCCCAAGT
β-actin	GTCTGCCTTGGTAGTGGATAATG	TCGAGGACGCCCTATCATGG

Note: SLC40A1: solute carrier family 40 member 1, F: forward sequence, R: reverse sequence.

values were then log2-transformed (log2(x + 0.001)) to obtain the expression profile and assess the prognostic influence of SLC40A1 in HNSC.

Research subjects

The study included 102 patients with NPC (NPC group), 97 individuals with AH (AH group), and 101 healthy controls. All participants were admitted and diagnosed at Hebei Eye Hospital between October 2021 and October 2023.

Patient selection (NPC and AH patients): Inclusion criteria: (1) Diagnosis of NPC (pathological stage: Tumor 1-2, Node 0-1, Metastasis 0 [T1-2N0-1M0]) or AH confirmed through nasopharyngoscopy with biopsy [17]; (2) Age ≥18 years; (3) Availability of complete medical record information. Exclusion criteria: (1) Presence of other malignancies, cardiac or hepatic disorders, or immune diseases; (2) Mental or cognitive impairments.

Healthy controls: Inclusion criteria: (1) Healthy individuals undergoing physical examinations at the hospital. (2) Age ≥18 years; (3) Availability of complete medical record information; (4) Normal physical examination results; (5) No significant past medical history; (6) Absence of chronic inflammatory or autoimmune diseases. The exclusion criteria were the same as for the patient groups.

Sample collection

Frozen nasal mucosal tissue and blood samples were collected from both the NPC and AH groups, along with blood samples from healthy controls.

Polymerase chain reaction (PCR)

Total RNA was extracted from each group of samples using the Trizol method. Subsequently, cDNA was synthesized from the total RNA using a reverse transcription kit. PCR was then performed to detect SLC40A1 expression in both tissue and blood samples. The reaction mixture consisted of 10 μL of Super SYBR Mix, 1 μL each of upstream and downstream primers (10 μmol/L), 2 μL of cDNA, and 6 μL of double distilled water. The PCR conditions were as follows: an initial pre-denaturation at 95°C for 3 minutes, followed by 40 cycles of denaturation at 95°C for 30 seconds, annealing at 56°C for 30 seconds, and extension at 71°C for 30 seconds. The primer sequences were designed by Nanjing GenScript Biotech Corporation (see **Table 1**), with beta-actin serving as the internal control. The relative expression levels were calculated using the $2^{-\Delta\Delta CT}$ method.

Western blot

Tissue samples were homogenized using radioimmunoprecipitation assay lysate and centrifuged to obtain the supernatant. Serum samples were centrifuged at 4°C (12,000×g, 10 min) to remove impurities. After determining protein concentration using the bicinchoninic acid method, the sample volume was adjusted (30 μg for tissue, 20 μL for serum). Proteins were separated using 10% sodium dodecyl sulfate polyacrylamide gel electrophoresis and then transferred to polyvinylidene fluoride membranes by wet electroblotting.

Blocking and incubation: The membranes were blocked with 5% skimmed milk for 1 hour. The primary antibody (anti-SLC40A1, 1:1000, ab239511, Abcam, USA) was applied overnight at 4°C, followed by three washes with tris-buffered saline with tween 20. The horseradish peroxidase-conjugated secondary antibody (1:5000) was incubated at room temperature for 1 hour.

Detection and quantification: Enhanced chemiluminescence was utilized for development, and the grayscale intensity of the bands was quantified using ImageJ software, with glyceraldehyde 3-phosphate dehydrogenase as the internal control.

EBV testing

Qualitative testing (enzyme-linked immunosorbent assay-based method): venous blood samples (typically 5-10 ml) were collected from

each patient and allowed to clot at room temperature for 30 minutes, followed by a 10-minute centrifugation at 3000 rpm. According to the kit instructions, the diluted serum sample was added to a microplate or reaction cup. Then enzyme-labeled anti-human immunoglobulin (Ig) M or IgG antibodies were added and incubated at 37°C for 30 minutes. A substrate solution was added, and color development was allowed to occur. The absorbance (OD) value is measured at 450 nm using an enzyme-linked immunosorbent assay reader. Samples exhibiting OD or relative light unit (RLU) value ≥ cutoff value were classified as positive; otherwise, it was considered negative. The cutoff value for OD was determined by calculating the mean OD of negative controls plus two standard deviations (SD) (Mean + 2 SD). In this study, OD ≥0.18 was judged as positive, while OD <0.18 was negative. The cutoff for RLU is calculated as Mean_RLU + 3×SD_RLU. Based on this criterion, samples with RLU ≥80 were categorized as positive, whereas readings <80 were negative.

Quantitative detection (quantitative PCR [qPCR]-based method): After plasma isolation, the samples underwent the following treatments: addition of sample lysis buffer to lyse cells or viruses, binding of nucleic acids to columns or magnetic beads, washing, and elution to obtain purified EBV DNA. QPCR was performed to quantify the EBV DNA in the sample.

Follow-up

NPC patients were monitored for at least 1 year, with monthly visits during the first 6 months and every 2 months for the following 6 months after discharge. The follow-up cut-off date was December 2024. The prognostic survival and progression status of the patients were recorded. NPC progression is defined as tumor recurrence or metastasis.

Observation indicators

SLC40A1 expression was measured in both NPC and AH tissues. The diagnostic efficacy of SLC40A1 in differentiating between NPC and AH was also evaluated. Furthermore, the relationship between SLC40A1 and the pathological features of NPC was explored in-depth. Additionally, factors influencing NPC progression were analyzed, and a risk prediction model was developed based on these findings.

Statistical analysis

All statistical analyses in this study were conducted using SPSS 25.0 software. Qualitative data were presented as [n (%)], and the chi-square test was employed for comparisons. For quantitative data, the Shapiro-Wilk test was initially used to assess the distribution. Data with a normal distribution were expressed as (mean ± SD), denoted as ($\bar{x} \pm s$). Independent samples t-test was utilized for between-group comparisons, one-way analysis of variance was used for multiple group comparisons, and least-significant difference analysis was used for post hoc tests. For data with a non-normally distributed, results were presented as [median (interquartile range)], with comparisons between groups and among multiple groups conducted using Mann-Whitney U tests and Kruskal-Wallis H tests, respectively. Correlations were analyzed using the Pearson correlation coefficient. The diagnostic value was evaluated using the receiver operating characteristic (ROC) curve analysis. Logistic regression analysis was performed to identify significant factors. The Bootstrap method (with 1000 repeated sampling times) was used for internal validation of the logistic regression model, and the adjusted consistency index along with the 95% confidence interval (CI) were calculated. The Hosmer-Lemeshow goodness-of-fit test was utilized for model calibration. For survival and recurrence analyses, the Kaplan-Meier method and the Log-rank test were used. A *P*-value of less than 0.05 was considered statistically significant.

Results

Bioinformatics analysis of SLC40A1

This study was the first to investigate the expression status of SLC40A1 in NPC through bioinformatics analysis, which revealed that SLC40A1 was expressed at a low level in HNSC ($P<0.05$, **Figure 2A**). Prognostic analysis further revealed that SLC40A1 had no impact on the prognostic survival of HNSC patients ($P>0.05$, **Figure 2B**). When analyzing the correlation between clinical staging and gene expression, it is found that SLC40A1 demonstrated no significant association with the N-stage (N0=220, N1=78, N2=205, N3=11) of HNSC ($P>0.05$). However, in the T-stage (T1=51, T2=157, T3=120, T4=189) and M-stage (M0=502, M1=5), a progressive decline in SLC40A1 expres-

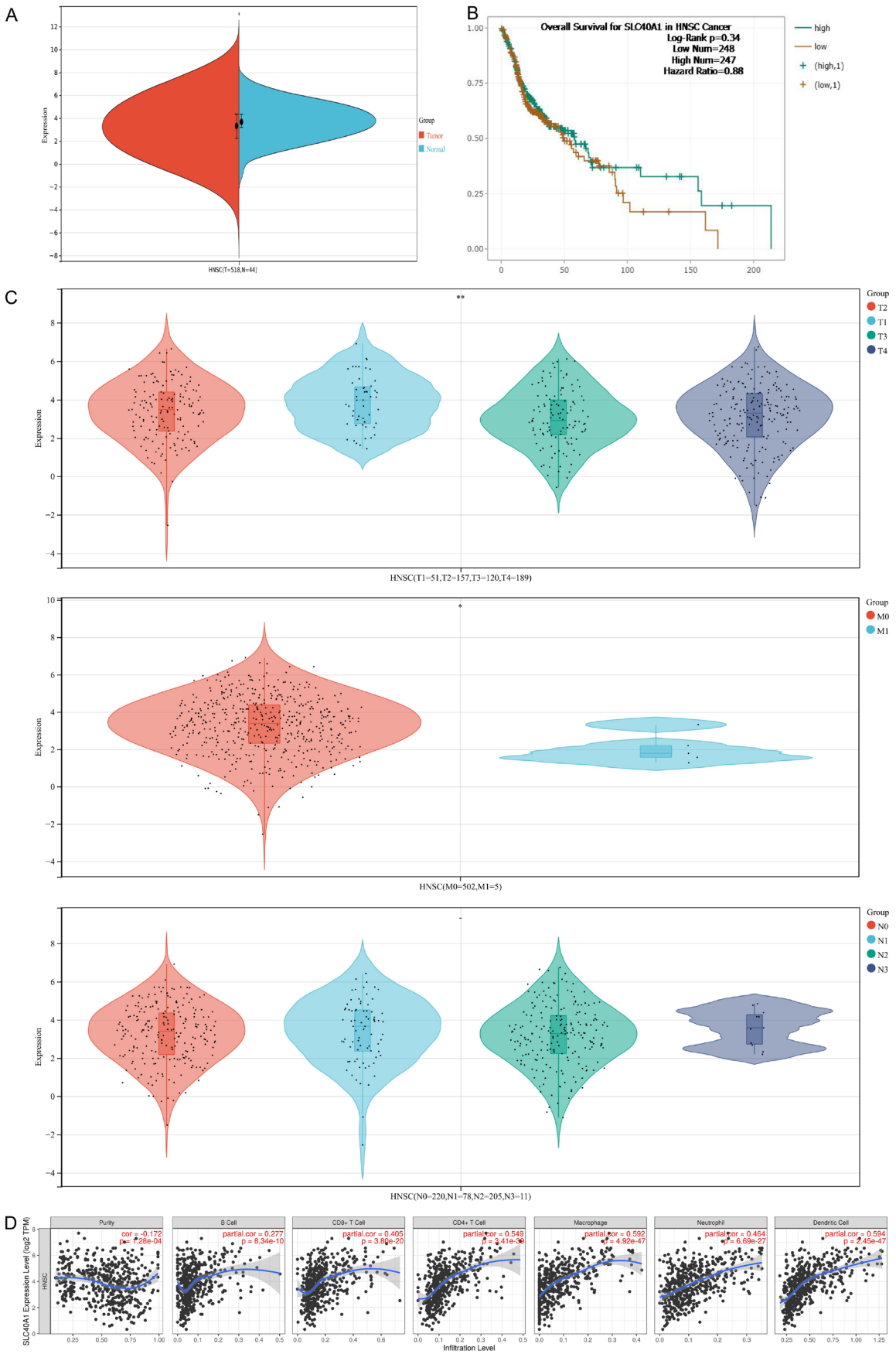
A
Expression
Group
Tumor
Normal
HNSC(T=518,N=44)
B
Overall Survival for SLC40A1 in HNSC Cancer
Log-Rank p=0.34
Low Num=248
High Num=247
Hazard Ratio=0.88
high
low
(high,1)
(low,1)
C
Group
T2
T1
T3
T4
HNSC(T1=51,T2=157,T3=120,T4=189)
Group
M0
M1
HNSC(M0=502,M1=5)
Group
N0
N1
N2
N3
HNSC(N0=220,N1=78,N2=205,N3=11)
D
Purity
B Cell
CD8+ T Cell
CD4+ T Cell
Macrophage
Neutrophil
Dendritic Cell
SLC40A1 Expression Level (log2 TPM)
Infiltration Level

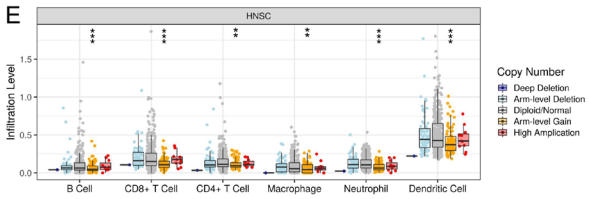

Figure 2. Bioinformatics analysis of SLC40A1. A. Bioinformatics analysis of the SLC40A1 expression. B. Bioinformatics analysis of the prognostic performance of SLC40A1. C. Bioinformatics analysis of the relationship between SLC40A1 and TNM staging of HNSC. D. Bioinformatics analysis of the relationship between SLC40A1 and HNSC immune cells. E. SCNA analysis of SLC40A1. Note: HNSC: head and neck squamous cell carcinoma, SLC40A1: solute carrier family 40 member 1, TNM: tumor node metastasis classification, SCNA: somatic copy number alteration, CD: cluster of differentiation.

Table 2. Comparison of clinical data

	Control (n=101)	AH (n=97)	NPC (n=102)	F (χ^2)	P
Age	64.90±4.55	64.81±5.20	63.24±5.20	0.267	0.766
Gender				1.007	0.604
Male	69 (68.32)	63 (64.95)	73 (71.57)		
Female	32 (31.68)	34 (35.05)	29 (28.43)		
Body mass index (kg/m^2)	21.95±2.42	22.50±3.58	22.82±2.64	2.293	0.103
Smoking				2.746	0.253
Yes	61 (60.40)	67 (69.07)	72 (70.59)		
No	40 (39.60)	30 (30.93)	30 (29.41)		
Drinking				2.765	0.251
Yes	35 (34.65)	44 (45.36)	37 (36.27)		
No	66 (65.35)	53 (54.64)	65 (63.73)		
Family history of AH				1.134	0.567
Yes	4 (3.96)	7 (7.22)	7 (6.86)		
No	97 (96.04)	90 (92.78)	95 (93.14)		
Family NPC history				2.018	0.365
Yes	2 (1.98)	4 (4.12)	6 (5.88)		
No	99 (98.02)	93 (95.88)	96 (94.12)		

Note: NPC: nasopharyngeal carcinoma, AH: adenoid hypertrophy.

sion was observed as the disease advanced (both P<0.05, **Figure 2C**). Additionally, in the analysis of the immune microenvironment, there was no obvious relationship between SLC40A1 and immune cells in HNSC (**Figure 2D**). However, in the somatic copy number alteration analysis, changes in the copy number of SLC40A1 still influenced the infiltration levels of all immune cells (**Figure 2E**), highlighting the important role of SLC40A1 in HNSC.

Comparison of clinical data

By statistically analyzing parameters such as age and gender across the NPC, AH, and control groups, the results showed no statistically significant differences among the groups (all P>0.05), indicating the comparability among research subjects (**Table 2**).

Clinical expression of SLC40A1

In tissue samples, SLC40A1 mRNA expression was lower in the neoplastic tissues than in the adjacent tissues in both the NPC and AH groups (both P<0.05, **Figure 3A** and **3B**). Additionally, SLC40A1 mRNA expression in the neoplastic tissues was substantially lower in the NPC group compared to the AH group (P<0.05, **Figure 3C**). Pearson correlation coefficient analysis indicated a positive correlation between SLC40A1 mRNA expression in the peripheral blood and neoplastic tissues of both NPC and AH patients (both P<0.05, **Figure 3D** and **3E**),

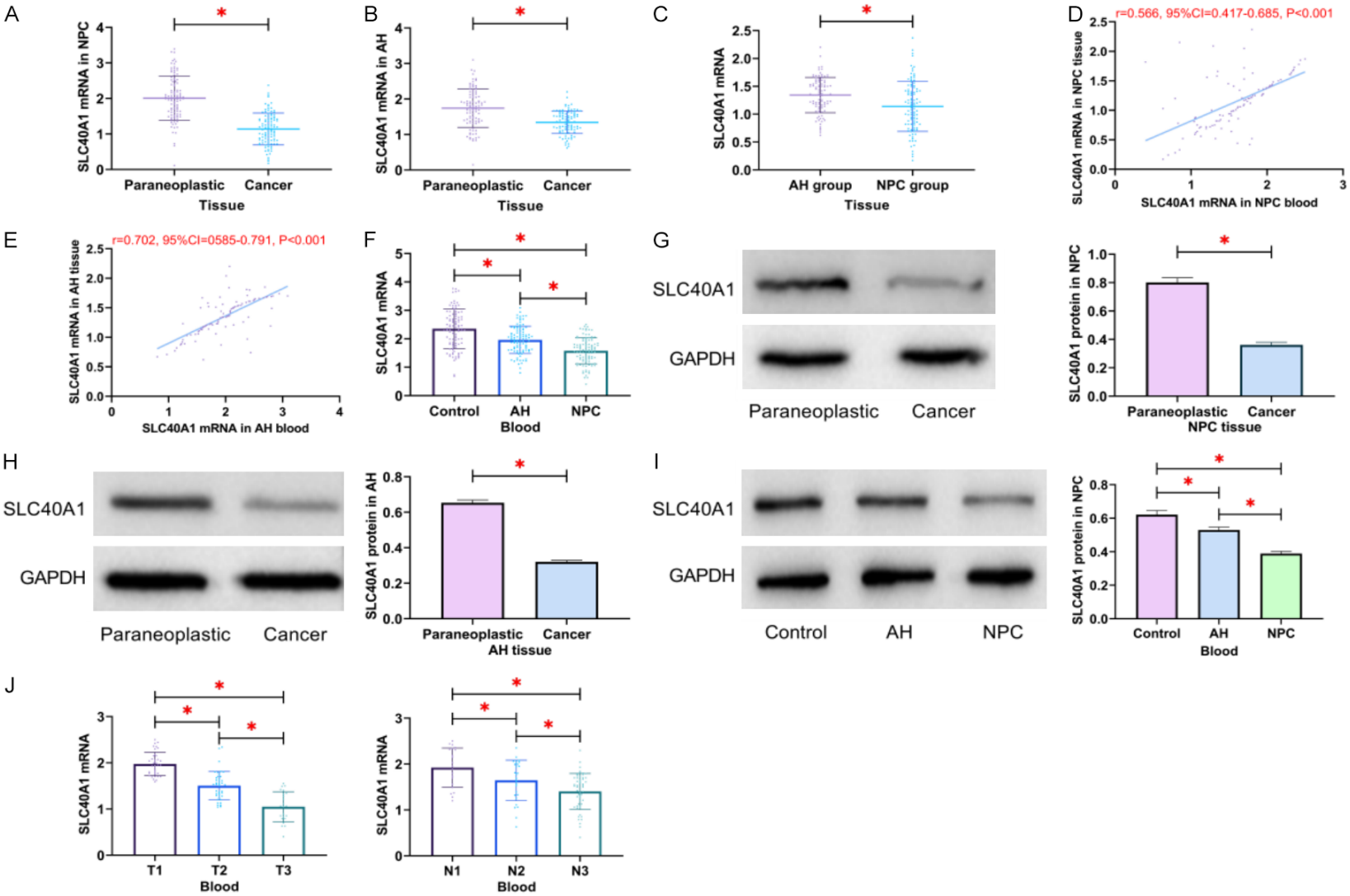

Figure 3. Clinical expression of SLC40A1. A. Comparison of SLC40A1 mRNA in NPC group. B. Comparison of SLC40A1 mRNA in AH group. C. Comparison of SLC40A1 mRNA in cancer tissues between the AH group and the NPC group. D. Correlation between SLC40A1 mRNA in NPC tissues and blood. E. Correlation between SLC40A1 mRNA in AH tissues and blood. F. Comparison of SLC40A1 mRNA in peripheral blood among control, AH, and NPC groups. G. Comparison of SLC40A1 protein in NPC tissues. H. Comparison of SLC40A1 protein in AH tissues. I. Comparison of SLC40A1 protein in peripheral blood among control, AH, and NPC groups. J. Comparison of SLC40A1 mRNA in NPC patients across different TNM stages. Note: *P<0.05. NPC: nasopharyngeal carcinoma, AH: adenoid hypertrophy, SLC40A1: solute carrier family 40 member 1, TNM: tumor node metastasis classification, GAPDH: glyceraldehyde-3-phosphate dehydrogenase.

Table 3. Association between SLC40A1 mRNA expression and the clinical features of NPC

	n	SLC40A1 mRNA	t	P
Age			0.309	0.758
≤63	58	1.59±0.43		
>63	44	1.56±0.50		
Gender			1.638	0.105
Male	73	1.62±0.48		
Female	29	1.46±0.38		
Body mass index (kg/m^2)			0.495	0.621
≤23	56	1.60±0.45		
>23	46	1.55±0.47		
Site of tumor			0.408	0.684
Pharyngeal Saphenous Fossa	47	1.60±0.44		
Parietal Wall	55	1.56±0.48		
Tumor diameter (cm)			1.403	0.164
≤5	54	1.64±0.46		
>5	48	1.51±0.44		
Number of lymph nodes			5.175	<0.001
1	64	1.74±0.43		
2 or more	38	1.31±0.38		
Lymph node size (cm)			4.300	<0.001
≤3	49	1.73±0.45		
>3	53	1.40±0.39		
Lymph node distribution			1.722	0.088
Unilateral	84	1.61±0.47		
Bilateral	18	1.41±0.38		
EBV infection			3.403	0.001
(+)	12	1.98±0.46		
(-)	90	1.52±0.43		

Note: NPC: nasopharyngeal carcinoma, SLC40A1: solute carrier family 40 member 1, EBV: Epstein-Barr virus.

demonstrating consistency. Regarding blood samples, the mRNA levels of SLC40A1 were higher in both the control and AH groups than those in the NPC group (both P<0.05, **Figure 3F**). Validation by Western blot further indicated lower SLC40A1 protein expression in cancer tissues versus paracancerous tissues in both the NPC and AH groups (both P<0.05, **Figure 3G** and **3H**). Multi-group comparison showed that the control group exhibited the highest serum SLC40A1 protein expression, followed by the AH group, with the lowest observed in the NPC group (all P<0.05, **Figure 3I**). Moreover, a subgroup analysis of SLC40A1 expression in the NPC patient cohort based on tumor node metastasis classification staging revealed that SLC40A1 expression levels decreased with increasing disease severity (all P<0.05, **Figure 3J**).

Association between SLC40A1 and the clinical features of NPC

To further investigate the relationship between SLC40A1 and NPC, the clinical characteristics of NPC patients were summarized. Comparative analyses revealed no notable differences in the mRNA expression of SLC40A1 among patients with different ages, genders, body mass index, sites of tumor, tumor diameters, or lymph node distributions (all P>0.05). Nevertheless, in patients with 2 or more lymph nodes and those with lymph sizes >3 cm, a significant reduction in the mRNA expression of SLC40A1 was observed (both P<0.05). In addition, SLC40A1 mRNA levels were significantly increased in patients with EBV infection (P<0.05) (**Table 3**).

Diagnostic efficacy of SLC40A1 for NPC

ROC curve analysis was conducted on the SLC40A1 mRNA expression in the blood samples of both the control and NPC groups. The results indicated that when the peripheral blood SLC40A1 mRNA level was below 2.16, the diagnostic sensitivity for NPC reached 90.20%, with a specificity of 62.38% (P<0.001; **Figure 4A**). Subsequently, we assessed the diagnostic performance of SLC40A1 for NPC in AH patients at the same cut-off value. When SLC40A1 mRNA was <1.82, its sensitivity for diagnosing NPC in AH patients was 73.53%, and the specificity was 63.92% (P<0.001, **Figure 4B**). Additionally, EBV is the most classic diagnostic marker for NPC. Correlation analysis revealed that SLC40A1 mRNA levels in NPC patients were negatively correlated with EBV DNA load (P<0.05, **Figure 4C**). Comparing the EBV DNA levels among the three study groups, the NPC group had the highest levels, while the control group had the lowest (both P<0.05, **Figure 4D**).

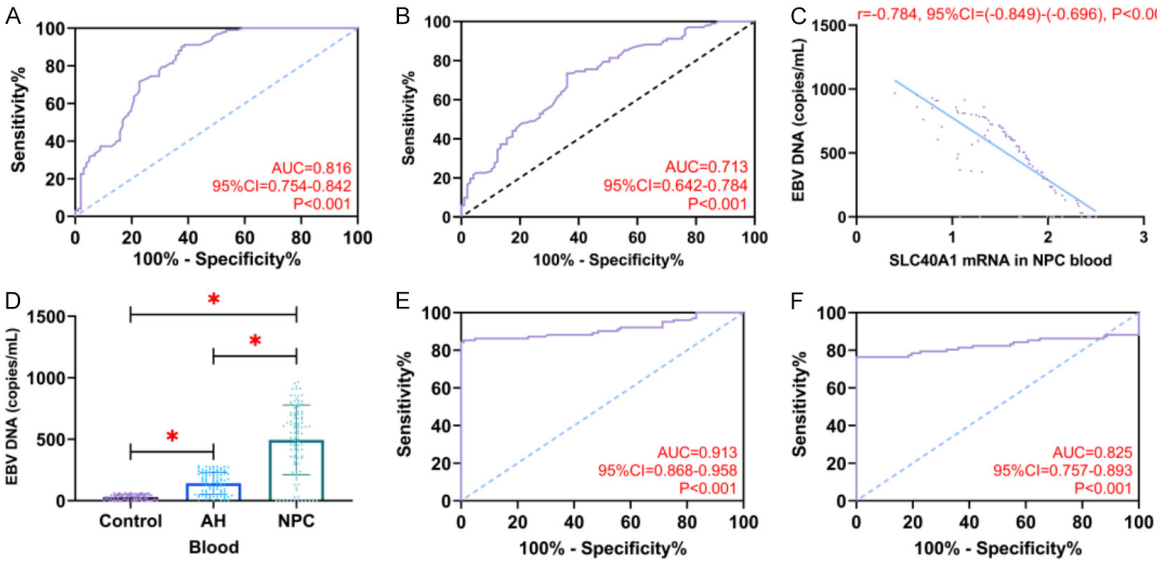

Figure 4. Diagnostic efficacy of SLC40A1 for NPC. A. ROC curve for the diagnosis of NPC in healthy controls by SLC40A1. B. ROC curve for the diagnosis of NPC in AH patients by SLC40A1. C. Correlation between SLC40A1 mRNA and EBV DNA. D. Comparison of the EBV DNA levels across the three study groups. E. ROC curve for identifying NPC in the general population by SLC40A1 with EBV DNA. F. ROC curve for identifying NPC in AH group by SLC40A1 with EBV DNA. Note: *P<0.05. ROC: receiver operating characteristic, NPC: nasopharyngeal carcinoma, AH: adenoid hypertrophy, SLC40A1: solute carrier family 40 member 1, AUC: aera under the curve, CI: confidence interval, EBV: epstein-barr virus.

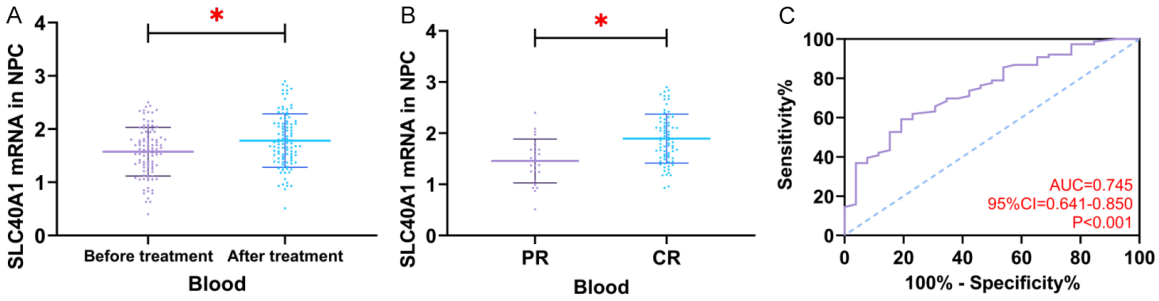

Figure 5. Prognostic efficacy of SLC40A1 for NPC. A. Changes in SLC40A1 before and after treatment in NPC group. B. Comparison of SLC40A1 in PR patients and CR patients after treatment. C. ROC curve of SLC40A1 for prognostic efficacy. Note: *P<0.05. SLC40A1: solute carrier family 40 member 1, ROC: receiver operating characteristic, CR: complete remission, PR: partial remission, NPC: nasopharyngeal carcinoma, AUC: aera under the curve, CI: confidence interval.

Logistic regression analysis yielded a formula for the combined detection of SLC40A1 mRNA and EBV DNA load for diagnosing NPC: In the general population, the sensitivity and specificity of diagnosing NPC using [Log(P) = -0.601 + (-0.747 × SLC40A1 mRNA) + 0.018 × EBV DNA] reached 84.00% and 100.00%, respectively (AUC=0.913, P<0.001, **Figure 4E**). In AH, the formula for distinguishing NPC [Log(P) = -2.113 + 0.001 × SLC40A1 mRNA + 0.008 × EBV DNA] achieved a sensitivity of 76.47% and a specificity of 100.00% (AUC=0.825, P<0.001, **Figure 4F**).

Prognostic efficacy of SLC40A1 for NPC

After treatment, SLC40A1 mRNA levels in NPC patients were significantly higher compared to pre-treatment levels (both P<0.05, **Figure 5A**), suggesting the potential of SLC40A1 for dynamic assessment in AH and NPC. Statistical analysis of radiotherapy and chemotherapy outcomes in NPC patients showed a complete remission rate of 84%. Compared to patients who achieved partial remission, those who achieved complete remission exhibited a more significant increase in SLC40A1 mRNA levels post-

Table 4. Univariate analysis of factors affecting the prognostic progression in NPC

	Non-progression (n=75)	Progression (n=24)	χ^2 (t)	P
Age			5.227	0.022
≤63	48 (64.00)	9 (37.50)		
>63	27 (36.00)	15 (62.50)		
Gender			0.282	0.596
Male	52 (69.33)	18 (75.00)		
Female	23 (30.67)	6 (75.00)		
Body mass index (kg/m^2)			1.498	0.221
≤23	42 (56.00)	10 (41.67)		
>23	33 (44.00)	14 (58.33)		
Site of tumor			0.183	0.669
Pharyngeal saphenous fossa	35 (53.33)	10 (41.67)		
Parietal wall	40 (52.33)	14 (58.33)		
Tumor diameter (cm)			10.372	0.001
≤5	47 (62.67)	6 (25.00)		
>5	28 (37.33)	18 (75.00)		
Number of lymph nodes			6.608	0.010
1	53 (70.67)	10 (41.67)		
2 or more	20 (29.33)	15 (58.33)		
Lymph node size (cm)			9.698	0.002
≤3	43 (57.33)	5 (20.83)		
>3	32 (42.67)	19 (79.17)		
Lymph node distribution			3.205	0.073
Unilateral	65 (86.67)	17 (70.83)		
Bilateral	10 (13.33)	7 (29.17)		
EBV infection			4.370	0.037
(+)	12 (16.00)	0 (0.00)		
(-)	63 (84.00)	24 (100.00)		
SLC40A1 mRNA	1.89±0.49	1.46±0.39	3.882	<0.001

Note: SLC40A1: solute carrier family 40 member 1, EBV: Epstein-Barr virus, NPC: nasopharyngeal carcinoma.

treatment (P<0.05, **Figure 5B**). The ROC curve showed that when post-treatment SLC40A1 mRNA levels exceeded 642.64, the sensitivity and specificity were 59.21% and 80.77%, respectively (AUC=0.745, P<0.05, **Figure 5C**). These findings provide valuable reference points for future clinical evaluations of radiotherapy and chemotherapy efficacy in NPC.

Analysis of factors associated with NPC prognosis

During the prognostic follow-up, we successfully tracked all NPC patients, with a mean follow-up time of 23.43±7.34 months. One patient died, resulting in an overall mortality rate of 2.94% (3/102). Additionally, disease progression was observed in 24 patients, yielding an overall progression rate of 24.24% (24/99). When comparing the clinical data of relapsed and non-relapsed patients, no significant differences were observed in factors such as gender and disease duration (all P>0.05). Nevertheless, patients in the progression group demonstrated higher values in terms of age, lymph node size, tumor diameter and the number of lymph nodes compared to the non-progression group; conversely, the SLC40A1 mRNA levels were lower in the progression group (all P<0.05). Meanwhile, there were more EBV-negative patients in the non-progression group (P<0.05) (**Table 4**). Subsequently, using the NPC progression status of the patients as the independent variable and the aforementioned differential indicators as covariates, a logistic regression analysis was conducted. The results indicated that EBV infection and the number of lymph nodes were not independent factors

Table 5. Assignment table

Factors	Assignment
Prognostic progress	Non-progression =1, Progression =2
Age	≤63=1, >63=2
Tumor diameter (cm)	≤5=1, >5=2
Number of lymph nodes	1=1, 2 or more =2
Lymph node size (cm)	≤3=1, >3=2
EBV infection	(-)=1, (+)=2
SLC40A1 mRNA	Use of raw data for analysis

Note: SLC40A1: solute carrier family 40 member 1, EBV: Epstein-Barr virus.

affecting NPC progression (both P>0.05). In contrast, tumor diameter, age, lymph node size, and tumor diameter were identified as independent risk factors for the prognostic progression of NPC, while SLC40A1 was found to act as a protective factor (P<0.05) (**Tables 5** and **6**).

Relationship between SLC40A1 and prognostic progression of NPC

Through ROC curve analysis, we found that when the SLC40A1 level was below 1.59, the diagnostic sensitivity for NPC progression was 66.67%, with a specificity of 76.00% (P<0.05, AUC=0.753, 95% CI=0.647-0.859). Based on the results of the aforementioned logistic regression analysis, a combined prediction model was established: Log (P) = -0.335 + (1.402 × Age + 1.512 × tumor diameter) + (1.504 × lymph node size) + (-2.024 × SLC40A1) (**Table 7**). Upon establishment, the model demonstrated a diagnostic sensitivity of 91.67% and a specificity of 72.00% for the prognostic progression of NPC (P<0.05, AUC=0.863, 95% CI=0.785-0.941, **Figure 6** and **Table 8**). To mitigate the risk of overfitting, the Bootstrap method was used for internal validation of the model. The results showed that the adjusted consistency index remained above 0.85, and the OR values of each variable were stable (**Table 7**).

Discussion

NPC represents one of the most common head and neck malignancies, with substantial implications for patient morbidity and mortality [18]. The clinical detection of early-stage NPC remains particularly challenging due to both its frequently asymptomatic presentation and symptom overlap with AH. Our investigation reveals a significant association between SLC40A1 and NPC, providing a preliminary analysis of its potential as a biomarker for NPC, which may ultimately facilitate earlier NPC detection and improve clinical outcomes.

Given that Zou et al. [12] remain the only group to have reported preliminary data on SLC40A1 in NPC, and considering the paucity of conclusive evidence in the literature, we initiated our investigation with comprehensive bioinformatics analyses. This approach enabled us to establish foundational insights into SLC40A1 expression patterns in NPC. The pan-cancer analysis revealed that SLC40A1 is downregulated in NPC, with its expression decreasing as the T-stage and M-stage advance. These results are consistent with those reported by Zou et al. [12], reinforcing the potential involvement of SLC40A1 in NPC pathogenesis. Subsequently, clinical sample analysis further confirmed these results, demonstrating that lower SLC40A1 expression was associated with larger tumor diameters, supporting its role in NPC pathogenesis and progression. Given the well-documented association between NPC and dysregulated iron metabolism, we hypothesized that this pathway may mediate SLC40A1's contribution to NPC pathogenesis. The iron efflux function of SLC40A1 plays a crucial role in ferroptosis regulation. Previous studies have demonstrated that SLC40A1 deficiency results in intracellular ferrous ion accumulation, GPX4-ROS axis activation, and lipid peroxidation induction [19]. The present study found that low SLC40A1 expression was associated with aggressive NPC phenotypes, potentially through ferroptosis inhibition. In contrast, while AH pathogenesis lacks established connections to iron metabolism, its development is known to involve recurrent nasopharyngitis-induced inflammation and immune dysregulation [20, 21]. Therefore, SLC40A1 may be involved in AH progression through these mechanisms. Although the downregulation of SLC40A1 in AH is less pronounced than in NPC, we identified its aberrant expression. However, there are other findings on SLC40A1 presenting contrary opinions. For instance, Feng et al. demonstrated that SLC40A1 was upregulated in ischemic cardiomyopathy, exacerbating mitochondrial dysfunction, oxidative stress, and apoptosis [22]. Liang et al. reported that knocking down SLC40A1 hindered the progression of prostate

Table 6. Multifactorial analysis of factors affecting the prognostic progression in NPC

	B	S.E.	Wald χ^2	P	OR	95% CI
Age	1.274	0.620	4.222	0.040	3.577	1.061, 12.063
Tumor diameter (cm)	1.512	0.627	5.823	0.016	4.537	1.328, 15.499
Number of lymph nodes	0.051	0.628	0.007	0.935	1.052	0.307, 3.602
Lymph node size (cm)	1.477	0.697	4.493	0.034	4.380	1.118, 17.163
EBV infection	19.003	>100.00	0.000	0.998	>100.00	-
SLC40A1 mRNA	-1.964	0.082	5.731	0.017	0.140	0.028, 0.700

Note: NPC: nasopharyngeal carcinoma, SLC40A1: solute carrier family 40 member 1, EBV: Epstein-Barr virus, B: regression coefficient, S.E.: standard error, OR: odds ratio, 95% CI: 95% confidence interval.

Table 7. Establishing a risk prediction model for NPC prognosis progression

	B	S.E.	Wald χ^2	P	Before correction		After correction	
					OR	95% CI	OR	95% CI
Age	1.402	0.611	5.262	0.022	4.062	1.226, 13.455	3.891	1.182, 12.764
Tumor diameter (cm)	1.512	0.617	6.015	0.014	4.538	1.355, 15.199	4.321	1.273, 14.658
Lymph node size (cm)	1.504	0.682	4.858	0.028	4.500	1.181, 17.143	4.187	1.134, 15.462
SLC40A1 mRNA	-2.024	0.749	7.306	0.007	0.132	0.030, 0.573	0.128	0.025, 0.638
Constant	-0.335	1.353	0.061	0.804	-	-	-	-

Note: NPC: nasopharyngeal carcinoma, SLC40A1: solute carrier family 40 member 1, B: regression coefficient, S.E.: standard error, OR: odds ratio, 95% CI: 95% confidence interval.

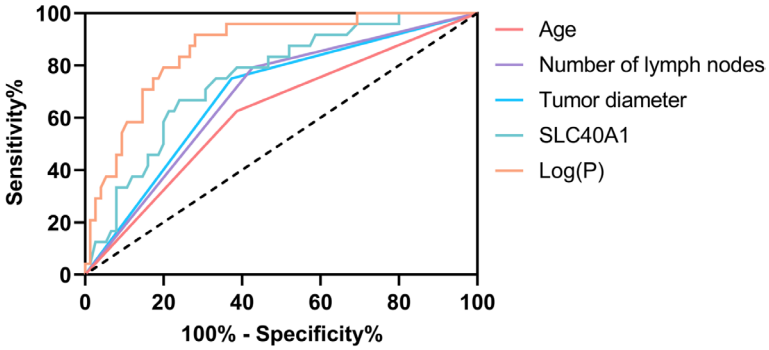

Figure 6. Relationship between SLC40A1 and prognostic progression of NPC. Note: NPC: nasopharyngeal carcinoma, SLC40A1: solute carrier family 40 member 1.

cancer [23]. These results suggest that SLC40A1 may exert its effects through different pathways in various diseases. The unique downregulation of SLC40A1 in NPC also underscores its potential as a future clinical biomarker for NPC.

It is well established that the current clinical diagnosis of NPC mainly relies on nasopharyngoscopy with biopsy. Despite its proven diagnostic accuracy, its invasive nature causes significant procedure-related stress in patients and poses challenges for large-scale clinical screening [24]. These limitations contribute substantially to the low detection rate of early-stage NPC. Our study revealed a consistent expression pattern of SLC40A1 in both tumor tissues and peripheral blood of NPC patients. Notably, SLC40A1 expression showed significant differences compared to both AH and control groups. These findings suggest SLC40A1's potential as a clinical biomarker for NPC. Specifically, peripheral blood SLC40A1 demonstrated excellent diagnostic performance, offering a novel and convenient approach for early NPC detection. Based on the differential expression patterns observed between AH and control groups, we propose that SLC40A1 could be integrated into routine clinical testing. Quantitative analysis against predetermined cutoff values could identify high-risk cases requiring further examination, potentially improving early diagnosis rate of NPC. This approach provides clinicians with a safe, non-invasive method to differentiate early-stage NPC from AH, which may ultimately improve patient outcomes. Supporting our findings, Zeng et al. identified SLC40A1 and TES as

Table 8. Relationship between SLC40A1 and prognostic progression of NPC

	AUC	95% CI	Sensitivity (%)	Specificity (%)	P
Age	0.619	0.490, 0.749	62.520	61.33	0.080
Tumor diameter (cm)	0.688	0.568, 0.808	75.00	62.67	0.006
Lymph node size (cm)	0.683	0.564, 0.801	79.17	57.33	0.007
SLC40A1 mRNA	0.753	0.648, 0.859	66.67	76.00	<0.001
Combined prediction model	0.863	0.785, 0.941	91.67	72.00	<0.001

Note: NPC: nasopharyngeal carcinoma, SLC40A1: solute carrier family 40 member 1, AUC: area under curve, 95% CI: 95% confidence interval.

potential prognostic markers in acute lymphoblastic leukemia through RNA-seq analysis [25], further underscoring SLC40A1's clinical potential.

Given the highly aggressive nature of NPC, patient prognosis remains a critical clinical consideration. While current treatments achieve >90% survival rates for early-stage NPC patients, disease progression still occurs in 12-24% of cases [26]. Our study observed a 2.94% mortality rate and 24.24% progression rate in the NPC cohort, consistent with previous reports. Multivariate analysis identified tumor diameter and the number of lymph nodes as independent risk factors for disease progression, in line with findings by Xu et al. [27]. Notably, SLC40A1 emerged as a protective factor against NPC progression, reinforcing its association with disease outcomes. These results suggest that therapeutic strategies activating SLC40A1 expression could potentially improve patient prognosis. This concept parallels work by Wu et al. [28], who proposed targeting SLC40A1 variants to treat erythroblastopenia. ROC analysis demonstrated SLC40A1's strong predictive value for NPC progression. Combining SLC40A1 with key prognostic factors, we developed a risk prediction model achieving 91.67% sensitivity and 72.00% specificity - performance metrics suggesting substantial clinical utility. These findings provide clinicians with novel tools for prognostic assessment in NPC management.

This investigation has several limitations that should be acknowledged. First, the relatively small sample size may introduce variability in the results. Second, as the study exclusively enrolled early-stage NPC patients, we could not examine potential associations between SLC40A1 expression and disease staging. While our findings suggest that SLC40A1 may influence EBV's lytic cycle through iron transport regulation - potentially via iron overload-mediated activation of EBV's BZLF1 gene promoter [13] - the precise mechanistic role of SLC40A1 in NPC pathogenesis remains unclear due to the absence of functional studies. Future research should (1) employ CRISPR-Cas9 to generate SLC40A1-knockout models for mechanistic studies; (2) assess mitochondrial function using Seahorse XF technology; (3) quantify expression of iron metabolism genes (e.g., FPN, FTL); (4) conduct large-scale clinical trials to validate SLC40A1's diagnostic utility in differentiating NPC from AH; (5) perform external validation of our risk prediction model using multicenter independent cohorts.

Conclusion

Our study demonstrates significant downregulation of SLC40A1 in NPC. The strong diagnostic performance of SLC40A1 suggests its potential as a novel, non-invasive biomarker for early NPC detection. These findings may provide clinicians with improved tools for prognostic evaluation and patient management, ultimately contributing to better clinical outcomes in NPC.

Acknowledgements

This work was supported by The Project of Xingtai Science and Technology Bureau (2022ZC177).

Disclosure of conflict of interest

None.

Address correspondence to: Chao Zhang, Hebei Eye Hospital, No. 399 Quanbei Street, Xiangdu District, Xingtai 054001, Hebei, China. E-mail: Hongwei840126@163.com

References

[1] Chen YP, Chan ATC, Le QT, Blanchard P, Sun Y and Ma J. Nasopharyngeal carcinoma. Lancet 2019; 394: 64-80.

[2] Carvajal F, Luyo G, Veloso J, Veloso M, Alarcon F, Villa E and Saavedra E. Advances in nasopharyngeal carcinoma treatment: induction chemotherapy and concomitant radio-chemotherapy. Rev Med Chil 2023; 151: 1221-1232.

[3] Limkin EJ and Blanchard P. Does East meet West? Towards a unified vision of the management of Nasopharyngeal carcinoma. Br J Radiol 2019; 92: 20190068.

[4] Cai M, Wang Y, Ma H, Yang L and Xu Z. Advances and challenges in immunotherapy for locally advanced nasopharyngeal carcinoma. Cancer Treat Rev 2024; 131: 102840.

[5] Jiang W, Zheng B and Wei H. Recent advances in early detection of nasopharyngeal carcinoma. Discov Oncol 2024; 15: 365.

[6] King AD, Wong LYS, Law BKH, Bhatia KS, Woo JKS, Ai QY, Tan TY, Goh J, Chuah KL, Mo FKF, Chan KCA, Chan ATC and Vlantis AC. MR imaging criteria for the detection of nasopharyngeal carcinoma: discrimination of early-stage primary tumors from benign hyperplasia. AJNR Am J Neuroradiol 2018; 39: 515-523.

[7] Feng Y, Xia W, He G, Ke R, Liu L, Xie M, Tang A and Yi X. Accuracy evaluation and comparison of 14 diagnostic markers for nasopharyngeal carcinoma: a meta-analysis. Front Oncol 2020; 10: 1779.

[8] Mao M, Sheng H, Tian B, Chi P, Huang K, Li H and Liu W. Significance of dynamic changes of VCA-IgA levels in pre- and post-treatment plasma of patients with nasopharyngeal carcinoma: development of a clinically-oriented model. Adv Ther 2023; 40: 2426-2438.

[9] Paudel S, Warner BE, Wang R, Adams-Haduch J, Reznik AS, Dou J, Huang Y, Gao YT, Koh WP, Backerholm A, Yuan JM and Shair KHY. Serologic profiling using an Epstein-Barr virus mammalian expression library identifies EBNA1 IgA as a prediagnostic marker for nasopharyngeal carcinoma. Clin Cancer Res 2022; 28: 5221-5230.

[10] Li XL, Bi HL, Yuan TJ and Huang YY. Diagnostic and prognostic values of KLK11 in nasopharyngeal carcinoma. Eur Rev Med Pharmacol Sci 2020; 24: 9423-9428.

[11] Zhang B, Xu B, Yu L, Pei Y and He Y. The diagnostic and prognostic value of plasma circulating CircNUP98 for nasopharyngeal carcinoma. Curr Mol Med 2024; 24: 226-232.

[12] Zou Z, Li R, Huang X, Chen M, Tan J and Wu M. Identification and validation of immune-related methylated genes as diagnostic and prognostic biomarkers of nasopharyngeal carcinoma. Head Neck 2024; 46: 192-211.

[13] Zhang Y, Zou L, Li X, Guo L, Hu B, Ye H and Liu Y. SLC40A1 in iron metabolism, ferroptosis, and disease: a review. WIREs Mech Dis 2024; 16: e1644.

[14] Mei J, Xiao X, Liang N, Dong L, Wei S, Mo L, Zhao W and Cai Y. Clinical significance of serum iron metabolism-related markers in patients with nasopharyngeal carcinoma. ORL J Otorhinolaryngol Relat Spec 2023; 85: 223-230.

[15] Su J, Zhong G, Qin W, Zhou L, Ye J, Ye Y, Chen C, Liang P, Zhao W, Xiao X, Wen W, Luo W, Zhou X, Zhang Z, Cai Y and Li C. Integrating iron metabolism-related gene signature to evaluate prognosis and immune infiltration in nasopharyngeal carcinoma. Discov Oncol 2024; 15: 112.

[16] Li HL, Deng NH, Xiao JX and He XS. Cross-link between ferroptosis and nasopharyngeal carcinoma: new approach to radiotherapy sensitization. Oncol Lett 2021; 22: 770.

[17] Du XJ, Wang GY, Zhu XD, Han YQ, Lei F, Shen LF, Yang KY, Chen L, Mao YP, Tang LL, Li L, Wu Z, Xu GQ, Zhou Q, Huang J, Guo R, Zhang Y, Liu X, Zhou GQ, Li WF, Xu C, Lin L, Chen YP, Chen FP, Liang XY, Chen SY, Li SQ, Cui CY, Li JB, Ren J, Chen MY, Liu LZ, Sun Y and Ma J. Refining the 8th edition TNM classification for EBV related nasopharyngeal carcinoma. Cancer Cell 2024; 42: 464-473 e3.

[18] Tang Y and He X. Long non-coding RNAs in nasopharyngeal carcinoma: biological functions and clinical applications. Mol Cell Biochem 2021; 476: 3537-3550.

[19] Xu P, Ge FH, Li WX, Xu Z, Wang XL, Shen JL, Xu AB and Hao RR. MicroRNA-147a targets SLC40A1 to induce ferroptosis in human glioblastoma. Anal Cell Pathol (Amst) 2022; 2022: 2843990.

[20] Ye C, Guo X, Wu J, Wang M, Ding H and Ren X. CCL20/CCR6 mediated macrophage activation and polarization can promote adenoid epithelial inflammation in adenoid hypertrophy. J Inflamm Res 2022; 15: 6843-6855.

[21] Schmidt A, Huber JE, Sercan Alp O, Gurkov R, Reichel CA, Herrmann M, Keppler OT, Leeuw T and Baumjohann D. Complex human adenoid tissue-based ex vivo culture systems reveal anti-inflammatory drug effects on germinal center T and B cells. EBioMedicine 2020; 53: 102684.

[22] Feng R, Wang D, Li T, Liu X, Peng T, Liu M, Ren G, Xu H, Luo H, Lu D, Qi B, Zhang M and Li Y. Elevated SLC40A1 impairs cardiac function and exacerbates mitochondrial dysfunction, oxidative stress, and apoptosis in ischemic myocardia. Int J Biol Sci 2024; 20: 414-432.

[23] Liang B, Cui S and Zou S. Leonurine suppresses prostate cancer growth in vitro and in vivo by regulating miR-18a-5p/SLC40A1 axis. Chin J Physiol 2022; 65: 319-327.
[24] Tang J, Chen H and Chen F. CT and MRI presentation of nasopharyngeal tuberculosis (with a case report). Radiol Case Rep 2024; 19: 1702-1707.
[25] Zeng X, Liu K, Xu R, Zhang L, Lai P, Du X and Weng J. TES and SLC40A1 as potential biomarkers for predicting survival in T-cell acute lymphoblastic leukemia. Acta Haematol 2025; 148: 163-179.
[26] Luo W. Nasopharyngeal carcinoma ecology theory: cancer as multidimensional spatiotemporal "unity of ecology and evolution" pathological ecosystem. Theranostics 2023; 13: 1607-1631.
[27] Xu P, Min Y, Blanchard P, Feng M, Zhang P, Luo Y, Fan Z and Lang J. Incidence of small lymph node metastases in patients with nasopharyngeal carcinoma: Clinical implications for prognosis and treatment. Head Neck 2017; 39: 305-310.
[28] Wu H, Ren X, Ge M, Dong P, Wang S, Yi H, Li X, Huo J, Zheng X, Gao M, Huang J, Zhang J, Wang M, Jin P, Nie N, Shao Y and Zheng Y. The novel SLC40A1 (T419I) variant results in a loss-of-function phenotype and may provide insights into the mechanism of large granular lymphocytic leukemia and pure red cell aplasia. Blood Sci 2021; 4: 29-37.